Identification of first and second layer aluminum atoms in dilute AlGaAs using cross-sectional scanning tunneling microscopy

Arthur R. Smith,[a] Kuo-Jen Chao, and C. K. Shih[b]
Department of Physics, The University of Texas at Austin, Austin, Texas 78712

K. A. Anselm, A. Srinivasan, and B. G. Streetman
Department of Electrical and Computer Engineering, The University of Texas at Austin, Austin, Texas 78712

(Received 6 October 1995; accepted for publication 28 June 1996)

Cross-sectional scanning tunneling microscopy is used to study dilute $Al_xGa_{1-x}As$ with $x=0.05$ to investigate the bonding configurations within this ternary alloy. Atomically resolved scanning tunneling microscopy images combined with symmetry considerations provide the assignment of first and second layer aluminum atoms. The Al–Al pair distribution function based on the experimental data is compared with the theoretical pair distribution function of a random alloy. While there exists a qualitative agreement, small deviations from the ideal random distribution are also found. © *1996 American Institute of Physics.* [S0003-6951(96)02235-8]

The method of cross-sectional scanning tunneling microscopy (XSTM) has advanced the exploration of the structural and electronic properties of cleaved cross-sectional semiconductor surfaces by enabling the direct imaging of electronic species such as dopant atoms and point defects[1–6] as well as the measurement of band structure and alloy composition across semiconductor heterostructures.[7–16] An important issue is whether or not a ternary alloy (such as AlGaAs) is random, as favored by entropy, or if instead it is ordered due to atomic-scale interactions during the growth process. To investigate this issue using XSTM requires the spatial identification of the individual substitutional sites of the ternary species (i.e., Al) within the alloy. Unfortunately, due to the complexity of the possible bonding configurations in the high concentration ternary alloy, it has been difficult to attain such a clear identification. Recently, however, identification of In bonding sites within low concentration ternary InGaAs has been achieved.[16] In this letter, we report an investigation of dilute AlGaAs with a nominal aluminum concentration of 5% and identify individual substitutional aluminum atoms in the first and second layers. We also calculate the pair distribution function from the measured data and compare it to the theoretical pair distribution function based on a randomly generated distribution of aluminum atoms.

All experiments are performed in an ultra-high-vacuum chamber with a base pressure of less than 4×10^{-11} Torr. STM tips used are polycrystalline W prepared using an electrochemical etching technique and then treated *in situ* using either field emission or electron bombardment. All samples are grown on top of GaAs (001) substrates using molecular beam epitaxy at 580 °C with *p*-type doping of 1×10^{19} cm^{-3} [Be]. Samples are cleaved *in situ*. The epilayer consists of repeated periods of AlGaAs/GaAs layers with nominal layer thicknesses of 200 Å.

Figure 1 shows a 300 Å by 230 Å XSTM image of an $Al_{0.05}Ga_{0.95}As$ region grown between GaAs regions. This image was acquired with a sample bias of -2.50 V and a tunneling current of 0.15 nA. Apparent heterojunction locations are marked by solid lines in Fig. 1. Throughout the image we see a variety of different features that are characteristic of the AlGaAs region. First of all, we see a large number of elongated bright features that we refer to as ''A'' in Fig. 1. Notably, the orientation of these A features is always the same relative to the underlying GaAs lattice. The second type of feature within the AlGaAs region is a single arsenic site that is slightly depressed relative to the surrounding arsenic atoms that we refer to as ''B'' in Fig. 1. The number of these B features is about the same as the number of A features. Since neither of these two features appears outside of the AlGaAs region, we conclude that these are aluminum atom related. There are also a number of what appear to be defect-related features within the AlGaAs region. For example, single arsenic vacancies appear towards the upper right of

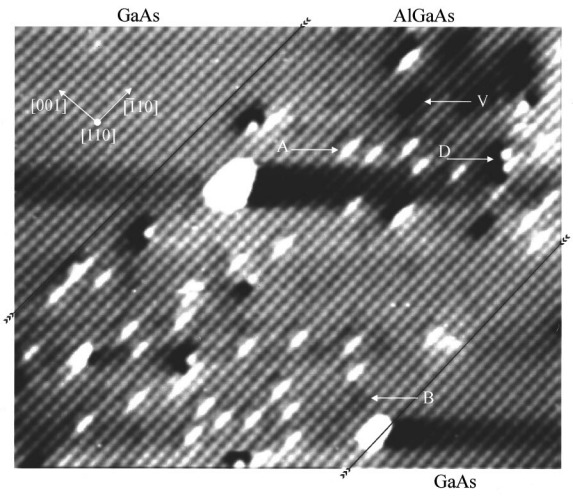

FIG. 1. 300 Å×230 Å filled-state STM images of GaAs/$Al_xGa_{1-x}As$/GaAs heterojunction region. The image was acquired with a sample bias of -2.50 V and a tunneling current of 0.15 nA. Approximate heterojuntion locations are indicated by black lines. ''A'' indicates a first layer aluminum atom feature while ''B'' indicates a second layer aluminum atom feature. Arsenic vacancies are indicated as ''V,'' and other defect related features are indicated as ''D.''

[a]Present address: Department of Physics, Carnegie Mellon University, Pittsburg, PA 15213.
[b]Author to whom all correspondence should be addressed.

 0003-6951/96/69(9)/1214/3/$10.00

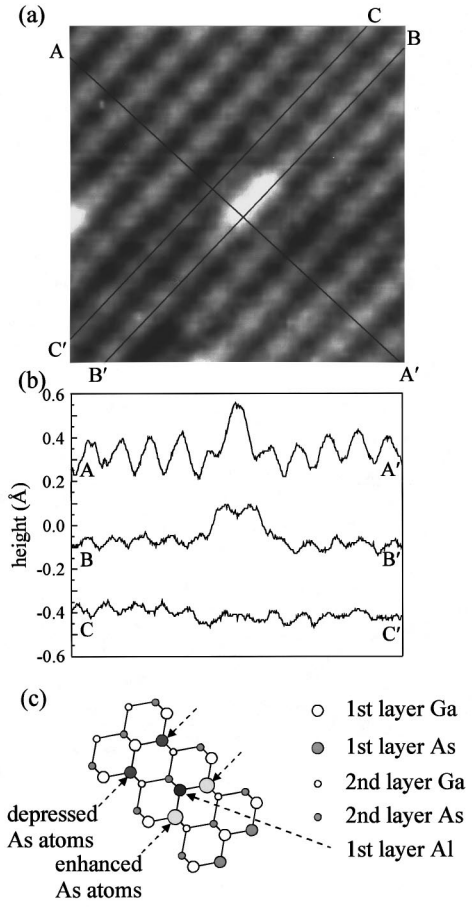

FIG. 2. (a) Zoom-in view of the first layer aluminum feature. (b) Line profiles taken across the feature from the points A, B, and C to the points A′, B′, and C′, respectively. Note that the lateral distance scales along the three line profiles are not exactly the same, but the vertical scales are the same. Line profiles have also been vertically shifted for clarity. (c) Atomic model of the region of the substitutional aluminum atom.

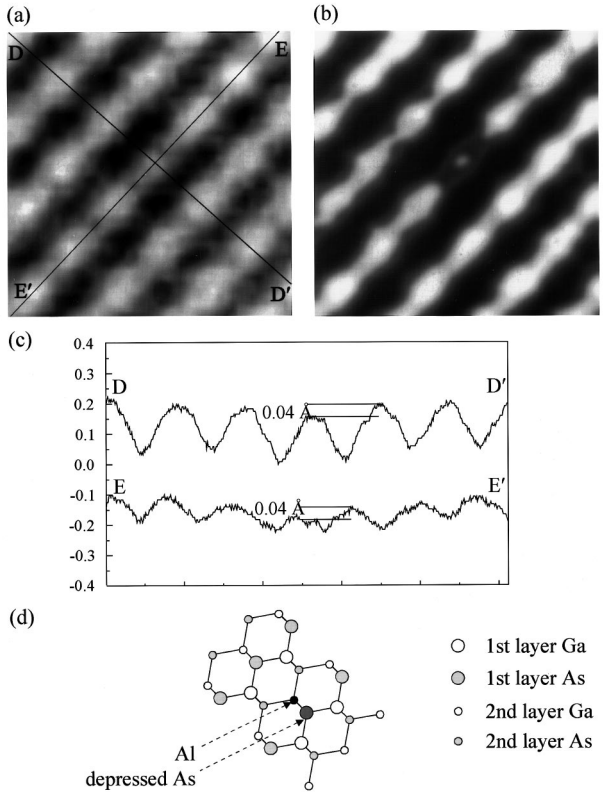

FIG. 3. (a) Zoom-in view of the back-bonded aluminum feature that is much easier to see in the gray-scale enhanced view shown in (b). Line profiles across the feature from the points D and E to the points D′ and E′ are shown in (c). The apparent depression due to the aluminum substitution is fairly weak, only about 0.04 Å. In (d) is shown an atomic bonding model for the back-bonded aluminum atom.

the image, indicated by ''V.'' In the analysis that follows below, we consider an area within the AlGaAs region that is relatively free of these defect-related features.

Shown in Fig. 2(a) is a zoom-in view of one of the A features. Not only does this feature consist of two enhanced arsenic atoms, but also two slightly depressed arsenic atoms, all of which are in almost perfect registry with the arsenic sublattice. The A feature has mirror symmetry about a [110] plane slicing through its center.

The symmetry is illustrated by the line cuts shown in Fig. 2(b). Since we are imaging the arsenic sublattice, it is straightforward to conclude that the A feature is only consistent with a substitutional atom occupying a first layer site of the gallium sublattice.

To pinpoint the exact location of the aluminum atom, is it useful to consider a simple model, as shown in Fig. 2(c). In this model, the relative orientation of the A feature and the GaAs lattice is based on an independent experimental determination. Even so, taking into account the symmetry of the A feature, there still remain two possible sites for the aluminum atom to occupy. For example, the aluminum atom may be on the zigzag chain containing the two depressed arsenic atoms, or it may be on the zigzag chain containing the two enhanced arsenic atoms. In the model, we have indicated that it is on the latter; however, conclusive proof would appear to require simultaneous imaging of the empty states, a more direct, but in practice, also more problematic approach.[17]

In our earlier work on AlAs/GaAs short period superlattices, we found that regions of pure AlAs appeared only dark relative to the GaAs regions in the filled state image[15] while in our current work, isolated aluminum atoms appear to have this bright/dark appearance. One possibility is that the surface Al atoms are decorated by certain residual gas such as hydrogen. Detailed calculations would be necessary in order to examine these possibilities. Nonetheless, the symmetry of the feature makes its identification as the effect of a first layer aluminum atom unmistakable.

The location of the second layer Al atom is totally unambiguous. Figure 3(a) is a zoom-in view of one of the dark sites indicated as B in Fig. 1. A nonlinear gray scale that enhances this feature is also shown in Fig. 3(b). Line profiles across the dark site show that it is only weakly depressed by about 0.03 Å relative to surrounding arsenic atoms, as shown in Fig. 3(c). Since only a single arsenic atom is affected, we know that it must be the effect of an aluminum atom occupying the back-bonded, second layer site of the gallium sublattice as shown in the model of Fig. 3(d).

Counting the number of these features within a certain area, we get a measure of the aluminum concentration. For a relatively defect-free AlGaAs region, we measure between 2% and 3% for both first and second layer aluminum atoms,

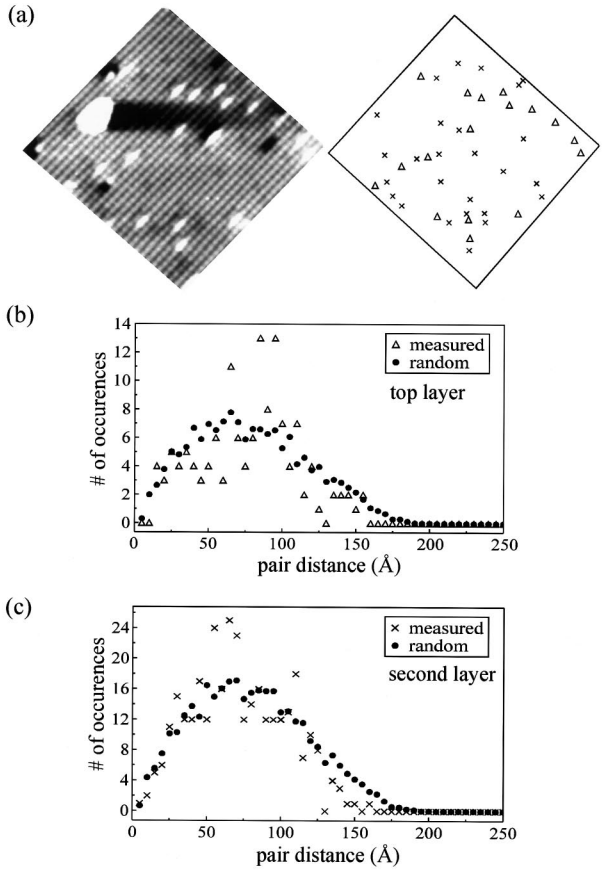

FIG. 4. (a) Schematic map of the aluminum atom locations for the area used in the pair distribution calculation. First layer aluminum atom locations are indicated by open triangles while second layer aluminum atom locations are indicated by x's. (b) Pair distribution histograms for the experimentally measured and randomly generated point distributions for the first layer aluminum atoms. The bin size is very 5 Å. This histogram is related to the pair distribution function by a probability normalization factor. (c) Similar pair distribution histograms for second layer aluminum atoms.

which is smaller than the nominal, intended concentration of 5%. However, this difference could be explained by error in the aluminum source deposition rate.

In order to address the question of whether or not the aluminum atoms are randomly distributed, we calculate the pair distribution function. This function is defined as the probability $p(r)$ of finding a pair of aluminum atoms separated by a certain distance r. $p(r)$ can be obtained from a given spatial distribution of aluminum atoms by calculating the distances between all possible pairs of aluminum atoms and plotting the results in the form of a histogram. In our analysis, we have calculated the results for first layer and second layer aluminum atoms separately for comparison.

For the calculation, we use an area of 30×30 lattice sites of the AlGaAs region of Fig. 1. Within this region, shown in Fig. 4(a), there are 17 first layer aluminum features labeled with open triangles. Calculating all possible pair distances results in 136 values; sorting these into bins, we then plot the pair distribution histogram in Fig. 4(b), also using open triangles for the plotting symbols. Filled circles represent the theoretical pair distribution histogram that is the average of 1000 histograms, each of which was calculated from a randomly generated distribution of aluminum atoms.

Similar analysis is performed for the 26 second layer aluminum atoms labeled in Fig. 4(a) with x's, which results in 325 pairs. The resulting pair distribution histogram is shown in Fig. 4(c) also using x's for the plotting symbols. The corresponding theoretical pair distribution histogram is shown in filled circles.

As can be seen, there is fairly good agreement between the experimental and random distributions. However, near the 150 Å pair distance, the experimental points dip slightly below the theoretical points while near the 75 Å pair distance, they rise slightly above them. Consistent for both the first and second layer, these deviations suggest an Al–Al interaction in the GaAs matrix. However, to be more conclusive on the nature of this interaction, a much larger experimental database would be required.

In conclusion, we have investigated bonding configurations of aluminum atoms within dilute AlGaAs using XSTM. Use of the dilute alloy enables us to identify features corresponding to isolated aluminum atoms in the STM images. First and second layer aluminum atoms have different effects on surface arsenic atoms, allowing us to differentiate between these two. Based on these assignments, the pair distribution function shows some deviations from ideal randomness that suggest the existence of Al–Al interactions in the GaAs matrix.

This work was supported by the National Science Foundation (Grant No. DMR-94-02938), a Texas Instruments University Research Grant, the Joint Services Electronics Program (Contract No. AFOSR F49620-92-C-0027), and the Science and Technology Center Program of the National Science Foundation (Grant No. CHE8920120). The authors also thank Dr. Ph. Ebert for useful discussions.

[1] Ph. Ebert, K. Urban, and M. G. Lagally, Phys. Rev. Lett. **72**, 840 (1994).
[2] J. F. Zheng, X. Liu, N. Newman, E. R. Weber, D. F. Ogletree, and M. Salmeron, Phys. Rev. Lett. **72**, 1490 (1994).
[3] M. B. Johnson, O. Albrektsen, R. M. Feenstra, and H. W. M. Salemink, Appl. Phys. Lett. **63**, 2923 (1993).
[4] G. Lengel, R. Wilkins, G. Brown, and M. Weimer, Phys. Rev. Lett. **72**, 836 (1994).
[5] G. Lengel, R. Wilkins, G. Brown, and M. Weimer, J. Vac. Sci. Technol. B **11**, 1472 (1993).
[6] K.-J. Chao, A. R. Smith, and C. K. Shih, Phys. Rev. B **53**, 6935 (1996).
[7] O. Albrektsen, D. J. Arent, H. P. Meier, and H. W. M. Salemink, Appl. Phys. Lett. **57**, 31 (1990).
[8] M. B. Johnson, U. Maier, H.-P. Meier, and H. W. M. Salemink, Appl. Phys. Lett. **63**, 1273 (1993).
[9] H. W. M. Salemink and O. Albrektsen, Phys. Rev. B **47**, 16 044 (1993).
[10] S. Gwo, K.-J. Chao, C. K. Shih, K. Sadra, and B. G. Streetman, Phys. Rev. Lett. **71**, 1883 (1993).
[11] A. R. Smith, S. Gwo, K. Sadra, Y. C. Shih, B. G. Streetman, and C. K. Shih, J. Vac. Sci. Technol. B **12**, 2610 (1994).
[12] R. M. Feenstra, D. A. Collins, D. Z.-Y. Ting, M. W. Wang, and T. C. McGill, Phys. Rev. Lett. **72**, 2749 (1994).
[13] A. Y. Lew, E. T. Yu, D. H. Chow, and R. H. Miles, Appl. Phys. Lett. **65**, 201 (1994).
[14] A. R. Smith, Kuo-Jen Chao, C. K. Shih, Y. C. Shih, and B. G. Streetman, Appl. Phys. Lett. **66**, 478 (1995).
[15] A. R. Smith, Kuo-Jen Chao, C. K. Shih, Y. C. Shih, A. Barr, and B. G. Streetman, J. Vac. Sci. Technol. B **13**, 1824 (1995).
[16] M. Pfister *et al.*, Appl. Phys. Lett. **67**, 1459 (1995).
[17] We note that most of the published STM images of AlGaAs are filled-state images. An exception to this is found in Ref. 9, above.